Metallography, Microstructure, and Analysis (2018) 7:48–56
https://doi.org/10.1007/s13632-017-0411-4

TECHNICAL ARTICLE

Thixoformability Analysis of 355 Aluminum Alloy

Leandro Cássio de Paula[1] · Gabriela Lujan Brollo[1] · Cecília Tereza Weishaupt Proni[1] · Eugênio José Zoqui[1]

Received: 8 August 2017 / Revised: 17 November 2017 / Accepted: 29 November 2017 / Published online: 22 December 2017

Abstract
SSM processing typically uses aluminum alloys with a high Si content as raw material. Alloys with a medium Si content, such as 355 (Al–5 wt.%Si–1.0 wt.%Cu–0.6 wt.%Fe–0.4 wt.%Mg), are extensively used in casting operations, but little is used in SSM applications. This study therefore sought to determine by thermodynamic, microstructural, and rheological evaluation whether a grain-refined 355 alloy is suitable raw material for thixoforming operations. Ingots were produced using a grain refiner (Al–5.0 wt.%Ti–1.0 wt.%B) and electromagnetic stirring. The thermodynamic behavior of the alloy was analyzed by means of thermodynamic simulation (Thermo-Calc®) and DSC at several heating rates. 355 semisolid slurry was then produced by reheating the alloy to 595 °C and partially melting it for 0, 30, 60, 90, and 120 s to produce a spheroidized microstructure, which was evaluated by optical microscopy. The rheological behavior of the slurry was evaluated by viscosity and stress measurements during thixoforging tests. The results show that the grain-refined 355 alloy is suitable for thixoforming as it has stable microstructural and rheological behavior over a broad temperature range in the semisolid state, a desirable characteristic for SSM processing control.

Keywords SSM processing · 355 alloy · Thixoformability · Thermodynamics · Microstructure · Apparent viscosity

Introduction

In semisolid materials (SSM) processing, which includes rheocasting and thixoforming, metal parts are processed in the mush state in the interval between the solidus and liquidus, where the slurry exhibits non-Newtonian, thixotropic rheology when sheared [1, 2]. The semisolid slurry is produced by cooling down the alloy from the liquid state until a 20–50% solid fraction is reached (a process called rheocasting) or by heating up the alloy from the solid state to a 30–60% liquid fraction (a process called thixoforming) [1–3]. SSM processing has many advantages over conventional metal forming and casting technologies, including the possibility of producing near-net-shape parts and smooth, laminar die filling, which eliminates the defects usually found in casting and requires only a fraction of the force used in conventional forming, so that material losses and process costs are lower [4, 5].

Since SSM processing was first developed, only two aluminum alloys, A356 and 357, have been used as raw material [6]. However, other important alloys, such as A332, have recently been investigated as potential candidates. Despite its high silicon content, A332 has been found to have satisfactory behavior similar to that of A356 alloy [7]. Recent research has shown that alloys previously considered problematic, such as near-eutectic and hypereutectic Al–Si–Cu alloys, are already considered strong candidates for application in semisolids [8]. Development of new alloys suitable for processing in the semisolid state is limited by the specific thermodynamic characteristics and interdependent microstructural and rheological properties of the semisolid slurry, which must allow forming in the semisolid state. Together these features determine what is known as the thixoformability of the material [9, 10].

The thermodynamic behavior of a candidate alloy for SSM processing can be evaluated using several thixoformability criteria available in the literature [9–13]. One such criterion is that the SSM working window should lie between the unstable eutectic knee (at lower liquid fractions) and the temperature at which the alloy has melted completely (higher temperatures) [11, 12]. Another important criterion in thixoformability analysis is that the

✉ Eugênio José Zoqui
zoqui@fem.unicamp.br

[1] Materials and Manufacturing Department, Faculty of Mechanical Engineering, University of Campinas – UNICAMP, Campinas, SP 13083-860, Brazil

liquid sensitivity, i.e., the variation in liquid fraction with temperature, should be less than 0.03 $°C^{-1}$ for satisfactory SSM process control [9–12].

The semisolid slurry can be evaluated morphologically by analyzing features such as grain size, primary-phase particle size (or globule size), and the circularity of these particles. The smaller and rounder the grains and primary-phase particles, the easier their relative movement under shear in the semisolid slurry, and hence, the more suitable the material is for SSM processing [1–5]. In thixoforming operations, a suitable microstructure can be obtained by controlled reheating of the alloy to the semisolid state and holding it in this condition (partial melting), a process that allows a particular combination of the diffusion effects associated with Ostwald ripening and coalescence to take place, until the ideal microstructure is achieved [14–17].

Finally, the rheological properties, which are intimately related to the microstructure of the semisolid slurry, can be evaluated by analyzing the viscosity behavior of the slurry as a function of shear rate and the stress behavior as a function of applied strain during SSM processing. Lower stress and viscosity values indicate a slurry with high thixoformability, which is desirable in SSM processing [16–19].

The 355 aluminum alloy tested here is a potential candidate for SSM processing as it is used extensively in the production of cast parts for the automotive industry. Despite its low Si content compared with other alloys in the 3XX.X series [10], 355 alloy has excellent mechanical properties. These are a result of the addition of small amounts of Cu and Mg to its composition, allowing it to be used in complex parts subjected to stress, such as cylinder heads, valve bodies, water jackets, union hose connectors, and several accessories for the construction and machine industries [20].

The present work discusses the use of 355 alloy in SSM processes. The thixoformability of the alloy, its microstructural evolution during partial melting and its rheological behavior during thixoforming are analyzed, and suitable processing parameters are identified. The study contributes to the very limited body of the literature on the use of 355 alloy in SSM processing, and the authors hope it will enable this alloy to be used on a wider scale in this type of processing.

Experimental Procedure

Table 1 shows the chemical composition of the 355 alloy used here. The composition was determined in a pure argon atmosphere with an optical spectrometer.

To evaluate the thixoformability of the alloy, thermodynamic simulation and thermal analysis were performed. For the former, Thermo-Calc® was used to determine the theoretical liquid-fraction versus temperature (f_L vs. T) curve for the alloy under the Scheil condition. Thermal analysis was carried out to determine the experimental f_L versus T curve using a differential scanning calorimeter (DSC) system. The samples (weight 50 g) were heated to 700°C at 5, 10, 15, 20, and 25°C/min. The heat flow rate and temperature were monitored with thermocouples. The f_L versus T relationship was determined with a thermal analysis software by applying the Flynn method of integration of partial areas under the DSC curves [21]. The liquid-fraction sensitivity (df_L/dT vs. T) was determined via derivation of the f_L versus T within this interval in order to evaluate the thixoformability of the alloy by the differentiation method [12].

The 355 alloy was melted and cast into a cylindrical refrigerated copper die measuring 30 mm (D) × 360 mm (H) at a pouring temperature of 670 °C (50 °C above the expected liquidus according to the numerical simulation). Since the addition of small quantities of titanium in solution as a grain refiner has proved promising in semisolid casting [22], 4 wt.% of Al–5.0 wt.%Ti–1.0 wt.%B master alloy was added and the melt was stirred electromagnetically with an induction coil around the casting die (8 kW, 60 Hz to produce a magnetic field of 14 gauss that is enough to promote the stirring but is not enough to increase the molten temperature) [23].

Semicircular samples measuring 15 mm (R) × 20 mm (H) were produced from the cast ingots and reheated at 100 °C/min to 595 °C (corresponding to a liquid fraction of close to 0.45 according to the numerical simulation) to form a semisolid slurry and held at this temperature for 0, 30, 60, 90, and 120 s. Reheating was performed in an 8-kHz 20-kW induction furnace with a 15-cm-internal-diameter, 10-cm-high coil. A type-K thermocouple was inserted in the center of the samples to measure the temperature. After the treatment, all samples were water quenched to keep their semisolid microstructure as unaltered as possible.

Table 1 Chemical composition of the 355 alloy tested (wt.%)

	Cu	Si	Mg	Zn	Fe	Mn	Ti	Al
Max.	1.50	5.50	0.6	0.35	0.60	0.50	0.25	Bal.
Min.	1.00	4.50	0.4	…	…	…	…	…
355	1.240	5.030	0.435	0.255	0.767	0.276	0.220	Bal.

Morphological characterization of the as-received alloy, the cast ingot, and the thermally treated samples was performed by optical microscopy. For the conventional (black and white) analysis, samples were ground and polished with a 0.4-µm diamond solution and then examined under a optical microscope fitted with an digital imaging camera to record primary globule size (GLS) and circularity shape factor (CSF). For the color metallography, the samples were etched electrolytically (1.8 ~ 2.0% HBF_4, 30 ~ 41 V, 0.2 ~ 0.4 A for 120–240 s) and examined under polarized light to record grain size (GS) [24]. GS and GLS were measured by the Heyn intercept method following ASTM E112-10 [23, 24]. Average globule CSF was determined with ImageJ 1.47 t software. The CSF can vary between 0 and 1, where 1 corresponds to a perfect circle.

To evaluate the rheological behavior under shear of the 355 slurry, semisolid cylindrical samples measuring 30 mm (D) × 30 mm (H) with a type-K thermocouple in the center were subjected to thixoforging tests after the reheating treatment and partial melting described earlier. The tests were performed in a compression rheometer with a maximum load capacity of 25 kN and two parallel circular plates that compress test specimens by moving in relation to each other. The maximum height reduction and compression rate are 85% and 125 m/s, respectively. The rheometer has a 25-kN capacity load cell (4–20 mA; 2 mv V^{-1}; ± 0.10% FRO) and an internal LVDT displacement sensor (range: 200 mm; repeatability: 2.5 linearity measurement; nonlinearity: ± 0.10% FRO) coupled to a data-acquisition system with a maximum sampling rate of 5000 samples per second. The stress versus strain and viscosity versus shear rate relationships were obtained for all the conditions analyzed with the aid of the Kirkwood and Laxmanan equations [1, 25], which can be found in Proni et al. [23] and Torres et al. [24].

Results and Discussion

Thermodynamic Characterization

Thermodynamic simulation using Thermo-Calc® under the Scheil condition for 355 alloy resulted in the liquid-fraction versus temperature curve (f_L vs. T) shown in Fig. 1. The letters in the graph indicate the temperature ranges in which the phase transformations occur during solidification. The phases are formed in the following order:

a. 621.5–619.4 °C: pure Al_{FCC} + Liq
b. 619.4–589.1 °C: Al_{FCC} + α + Liq
c. 589.1–565.7 °C: α + AlFeSi_β + Liq
d. 565.7–542.8 °C: α + AlFeSi_β + Si + Liq
e. 542.8–542.8 °C: α + AlFeSi_β + $Al_8FeMg_3Si_6$ + Si + Liq
f. 542.8–534.0 °C: α + $Al_8FeMg_3Si_6$ + Si + Liq
g. 534.0–515.8 °C: α + $Al_8FeMg_3Si_6$ + $Al_5Cu_2Mg_8Si_6$ Si + Liq
h. 534.0–515.8 °C: α + $Al_8FeMg_3Si_6$ + $Al_5Cu_2Mg_8Si_6$ + AlFeSi_β + Si + Liq
i. 515.8–513.8 °C: α + $Al_5Cu_2Mg_8Si_6$ + AlFeSi_β + Si + Liq
j. 513.8–505.9 °C: α + $Al_5Cu_2Mg_8Si_6$ + Al_7Cu_2Fe + Al_2Cu + Si + Liq

Note that Thermo-Calc® differentiates the pure Al_{FCC} from the α solid solution formed mainly of Al_{FCC} with Cu, Fe, Mg, Mn, and Si. However, in metallography, and for the purposes of thixoforming, these phases are indistinguishable. The expected liquidus and solidus are 621.5 and 505.9 °C, respectively.

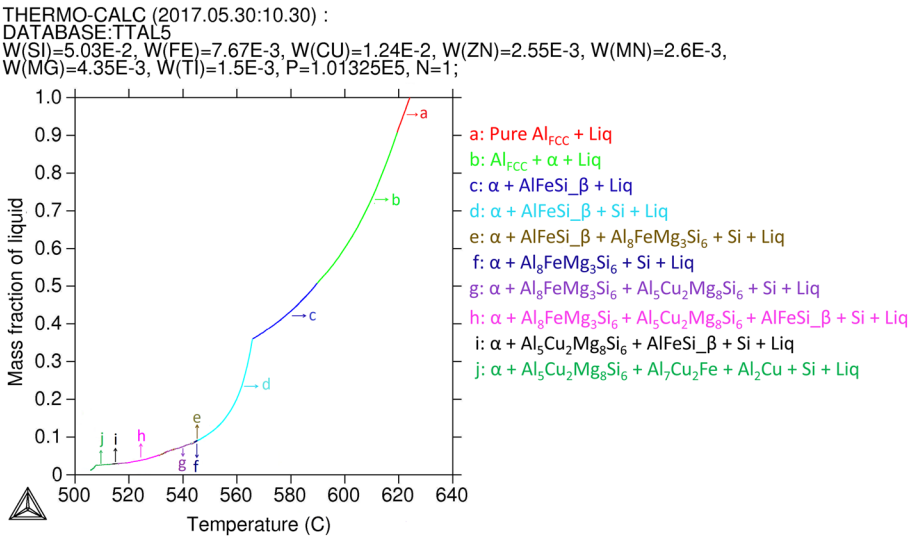

Fig. 1 Liquid-fraction versus temperature curves (f_L vs. T) obtained by numerical simulation (Scheil condition) for the 355 alloy. The letters a to j indicate phase transformations during solidification

The alloy was also characterized by DSC at several heating rates, and the results were then used with the differentiation method and Flynn method of integration of partial areas to produce the f_L versus T curves in Fig. 2a. The results of the numerical simulation under the Scheil condition (black curve) are also shown for reference purposes. The Scheil condition is the nearest to thermodynamic equilibrium of all the conditions analyzed. The higher the heating rate (i.e., the farther the process is from thermodynamic equilibrium), the more the phase transformations are delayed and the more they move toward higher temperatures (to the right), farther from the Scheil condition. As the heating rate increases, the semisolid interval becomes larger and the eutectic knee progressively smoother. This behavior has already been observed and discussed in Zoqui et al. [11] and Brollo et al. [12].

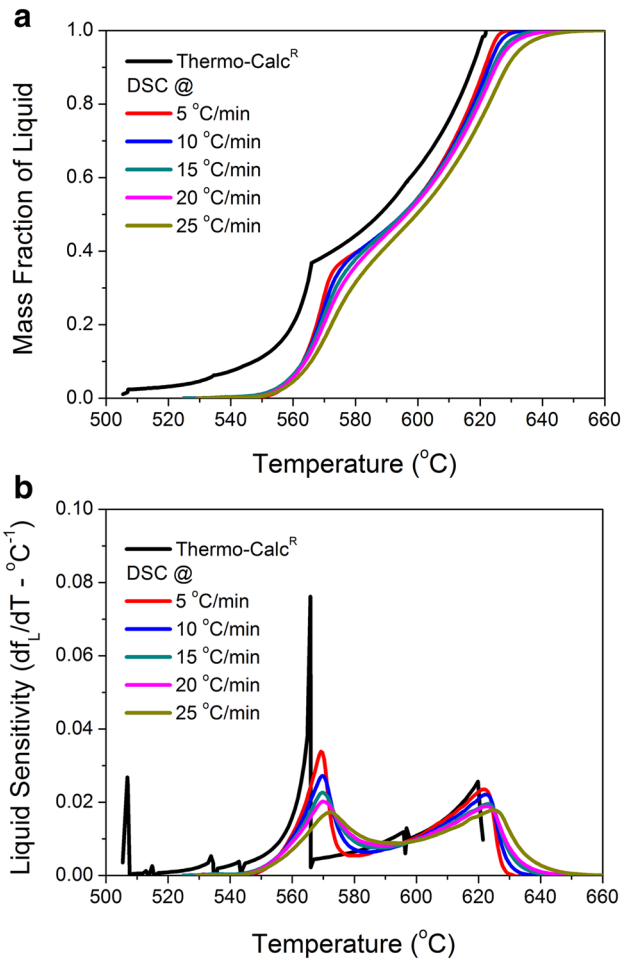

Fig. 2 Liquid-fraction (f_L vs. T) curves (**a**) and the corresponding liquid sensitivity (df_L/dT vs. T) curves (E.J.) for 355 alloy at heating rates of 5, 10, 15, 20, and 25°C/min. The curves for the numerical simulation (Scheil condition—dark black) are shown for reference purposes

The differentiation method was used to identify several temperatures of interest in thixoforming: the solidus (T_S), the eutectic knee (T_{Knee}), the upper and lower limits of the working window (T_{SSMI} and T_{SSMF}) and the liquidus (T_L). These temperatures are shown in Table 2 for all the heating conditions. A detailed discussion of how these parameters vary with thermodynamic and kinetic conditions can be found in Brollo et al. [12].

The sensitivity curves for all the heating cycles analyzed are shown in Fig. 2b. The results of the numerical simulation under the Scheil condition (black curve) are again shown for reference purposes. The features observed in the original f_L versus T curves are directly reflected in the differentiated curves: As the transformation becomes smoother and extends over a wider range with increasing heating rate, so the sensitivity decreases and the peaks become smaller and broader. The maximum sensitivity within the SSM working window (between T_{SSMI} and T_{SSMF}), which is used to analyze the thixoformability, is also shown in Table 2. The highest sensitivity for each experimental working window was below the stipulated limit of 0.030 $°C^{-1}$. The highest value was only 0.023 $°C^{-1}$ (for a heating rate of 5 °C/min). Thus, the SSM working window suggested by the differentiation method was maintained for all the conditions analyzed.

Considering the thermodynamic features of the alloy described above and the proposed working windows for the various conditions analyzed, a target temperature of 595 °C was chosen to evaluate the microstructural and rheological behavior of the alloy in the semisolid state. This temperature should correspond to a liquid fraction of 0.57 according to

Table 2 The solidus (T_S), eutectic knee (T_{Knee}), working window (T_{SSMI} and T_{SSMF}), and liquidus (T_L) for 355 alloy in the SSM processing interval and the corresponding liquid fractions (f_{Knee}, f_{SSMI}, f_{SSMF}) and maximum sensitivity determined by simulation (Scheil condition) and DSC

Rate (°C/min)	T_S (°C)	T_{Knee} (°C)	f_{Knee}	T_{SSMI} (°C)	f_{SSMI}	T_{SSMF} (°C)	f_{SSMF}	T_L (°C)	df_L/dT_{max} ($°C^{-1}$)
Scheil	505.9	566.8	0.37	568.0	0.38	621.2	0.95	621.5	0.026
5	524.6	573.8	0.35	581.3	0.40	623.4	0.94	636.3	0.023
10	524.8	574.1	0.35	586.6	0.44	622.3	0.89	648.6	0.021
15	524.8	573.4	0.34	588.4	0.45	622.3	0.87	649.3	0.019
20	529.1	574.8	0.42	589.8	0.44	622.3	0.86	657.8	0.018
25	529.1	577.1	0.42	592.1	0.43	624.6	0.84	664.1	0.017

Thermo-Calc® or approximately 0.5 according to DSC, each with very low liquid-fraction sensitivities (0.011 $°C^{-1}$ and approximately 0.009 $°C^{-1}$, respectively). Successful thixoforming can therefore be expected at this target temperature, as all the data collected show that the semisolid working windows occur between 568.0 and 624.6 °C or, in the worst-case scenario, 592.1 and 621.2 °C.

Microstructural Characterization

Figure 3 shows the microstructure of the as-received 355 alloy. Figure 3a is a conventional black and white (B&W) micrograph and shows the coarser α phase surrounded by the eutectic phase. The grain structure is not recognizable in this micrograph, but the real size (1.13 ± 0.43 mm) and complexity of the grain can be observed in the polarized color micrograph in Fig. 3b. The microstructure indicates that the as-received material can be considered non-thixoformable, as even though melting starts at the grain boundary and liquid continues to form as the eutectic inside the grain melts, the large, complex microstructure will remain solid in the semisolid temperature range. Large, complex structures like that observed here have a skeleton that impairs semisolid processing and require refining before they can be used for thixoforming.

Figure 4 shows the alloy after melting and casting in a refrigerated copper mold with electromagnetic stirring and the addition of chemical grain refiner. The B&W micrograph (Fig. 4a) shows the same α phase surrounded by the eutectic, but the effect of refining is clear. The structure is highly refined, and the eutectic is distributed homogenously. The coarse dendritic microstructure has been replaced by a rosette-like morphology where the primary-phase particle size (which is in fact the dendrite cell size) is 38 ± 7 µm.

The effect of grain refining is also evident in the grain structure in Fig. 4b, where the grain size has decreased considerably to 136 ± 28 µm, giving a ratio GS/GLS = 3.56 ± 0.95. The CSF remains very low (0.26 ± 0.13), and heat treatment in the semisolid state for seconds or, in some cases, minutes is needed to ensure adequate spheroidization.

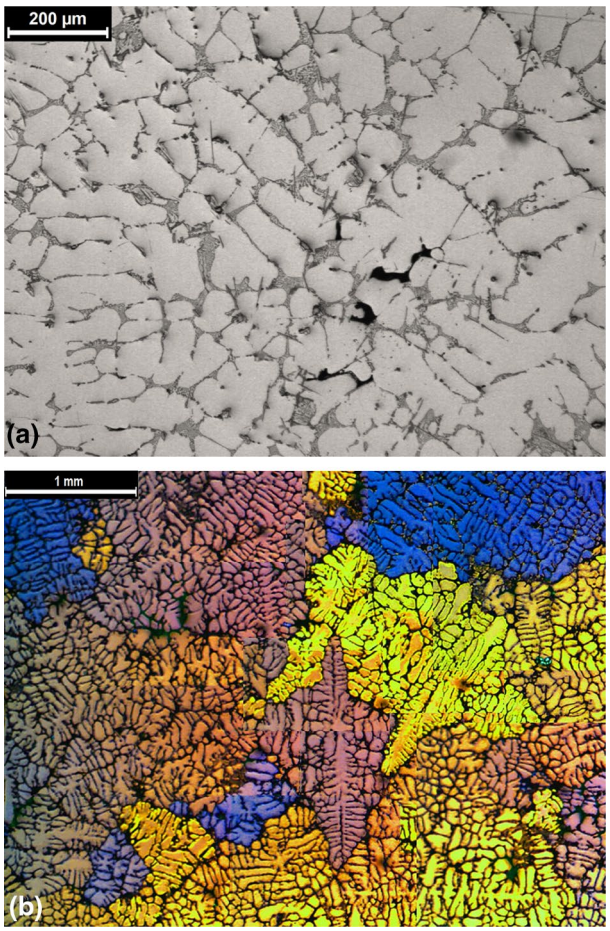

Fig. 3 Microstructure of the as-received 355 showing the primary phase and eutectic (**a**) and the grain morphology (**b**)

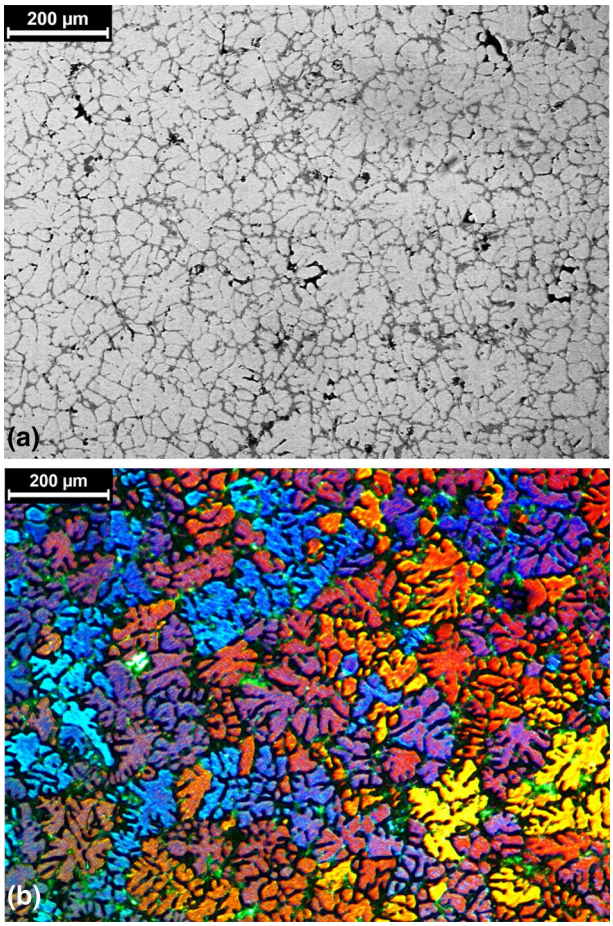

Fig. 4 Microstructure of the as-cast, grain-refined 355 alloy: grains (**a**) and primary-phase particles (**b**)

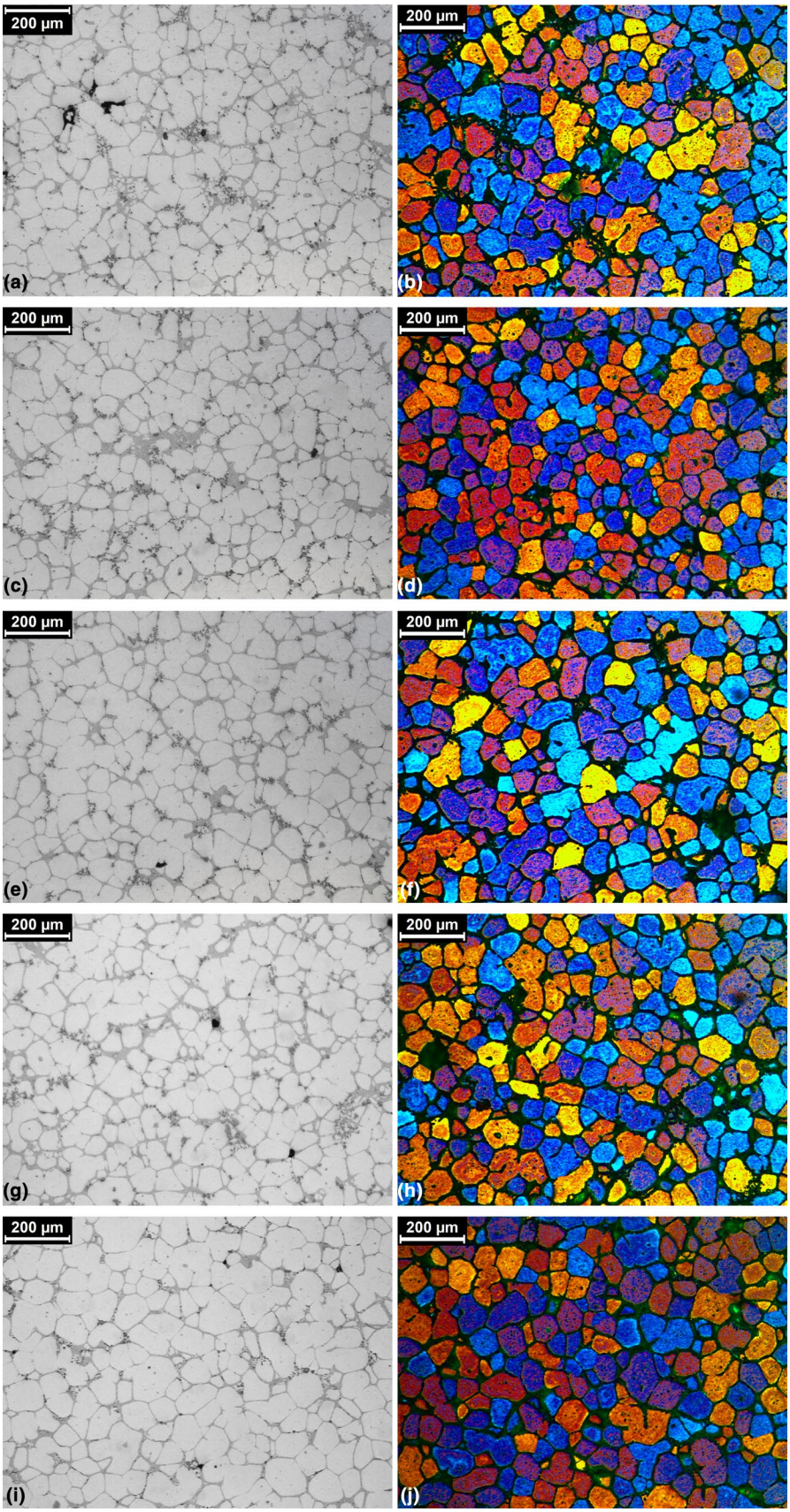

Fig. 5 Conventional black and white metallography showing the primary-phase structure and polarized color metallography showing the grain morphology in the reheated, partially melted 355 alloy for holding times of 0 s (**a**, **b**), 30 s (**c**, **d**), 60 s (**e**, **f**), 90 s (**g**, **h**), and 120 s (**i**, **j**) at 595 °C

Table 3 Grain size (GS), globule size (GLS), circularity shape factor (CSF), and rheocast quality index (RQI) for 355 alloy for all the conditions tested

Condition	GS (μm)	GLS (μm)	CSF	RQI GLS*CSF/GS
As cast	136 ± 28	38 ± 7	0.26 ± 0.13	0.07 ± 0.04
0 s	122 ± 28	73 ± 12	0.55 ± 0.19	0.33 ± 0.15
30 s	119 ± 33	74 ± 12	0.58 ± 0.19	0.36 ± 0.16
60 s	112 ± 29	78 ± 14	0.59 ± 0.19	0.41 ± 0.18
90 s	110 ± 20	77 ± 11	0.59 ± 0.18	0.41 ± 0.16
120 s	119 ± 24	77 ± 13	0.62 ± 0.19	0.40 ± 0.16

Figure 5 shows the microstructure of the alloy after reheating and partial melting. The effect of temperature and holding time on the primary-phase particle size and grain morphology of the as-cast alloy is apparent. The rosette-like morphology of the as-cast alloy has been replaced by a globular microstructure, a change usually associated with Ostwald ripening, which predominates when heating starts, followed by coalescence, which predominates during holding. In general, all the microstructures are well refined and globular.

Figure 5a, c, e, and g shows that, with the exception of the 120-s holding time, holding in the semisolid state produces few significant changes in the size or shape of the primary-phase particles, which can now be referred to as globules. The longest holding time (120 s) results in greater coarsening, and the structure becomes less globular. The eutectic phase surrounding the primary-phase boundaries is well distributed, but the extent of any possible interconnections in the structure cannot be determined. These interconnections must be broken in the semisolid state to achieve low-viscosity flow.

Similar observations can be made for the color micrographs taken using polarized light, where the grain structure can be observed. Holding times of 30–90 s (Fig. 5d, f, h) lead to a high degree of spheroidization without a significant grain growth, but at 120 s (Fig. 5j) the grain becomes larger. Heating up to the semisolid state with a holding time of 0 s (Fig. 5b) does not produce a well-refined, globular structure.

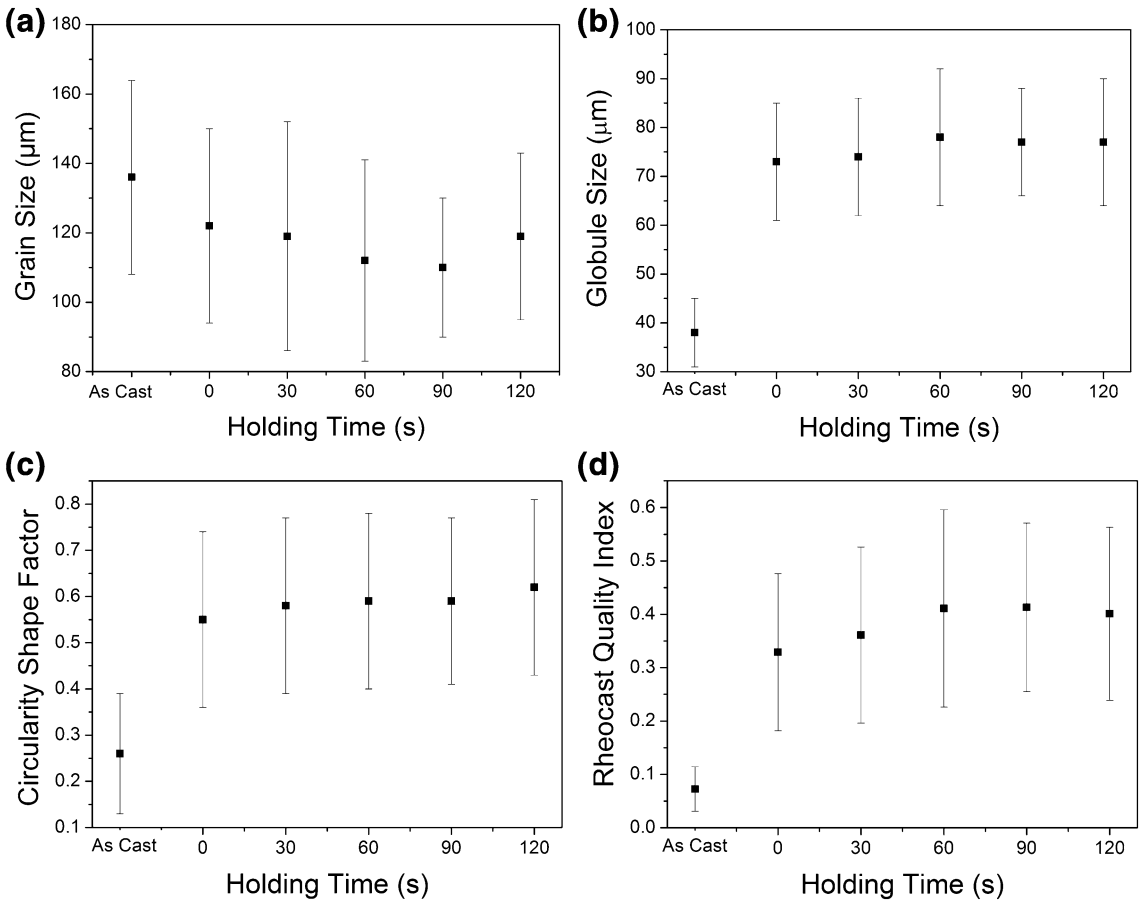

Fig. 6 Grain size (GS) (**a**), globule size (GLS) (**b**), circularity shape factor (CSF) (**c**), and rheocast quality index (RQI) (**d**) as a function of holding time at 595 °C for 355 alloy

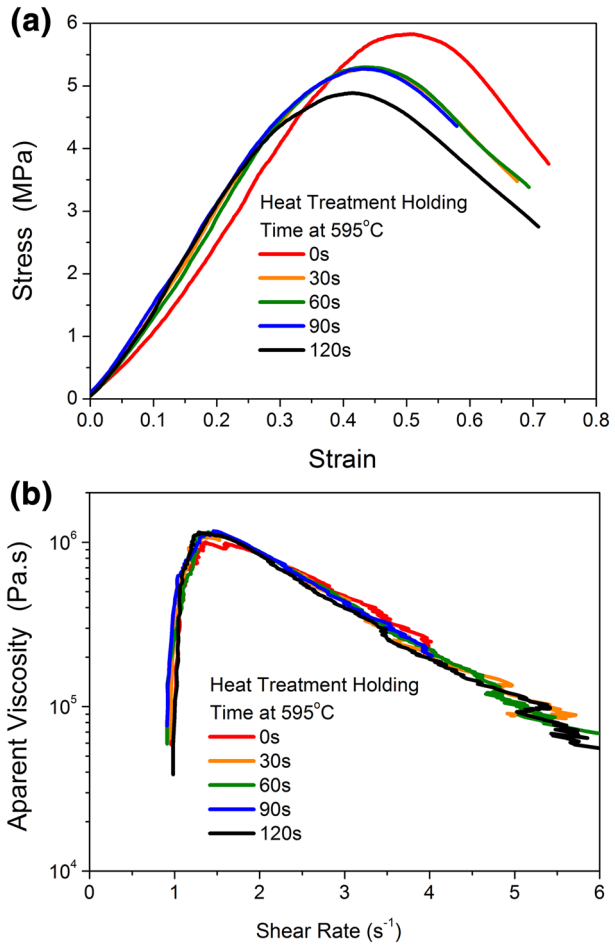

Fig. 7 Stress versus strain curves (**a**) and apparent viscosity versus shear rate curves (**b**) for 355 alloy during thixoforming at 595 °C after partial melting for different holding times

While qualitative examination of the micrographs suggests that the heat-treated material is fully globular for all the holding times, it is not possible to assert that long holding times are more effective in this regard than short ones, as only quantitative metallography can determine the true complexity of the microstructure.

Table 3 shows the mean GS, GLS, and SF (and corresponding standard deviations) for the alloy in the as-cast form and after the different heat treatments analyzed (reheating and partial melting). Heat treatment has led to a significant improvement in the microstructure, with smaller grains, rounder globules, and a more homogeneous structure. This is reflected in the rheocast quality index (RQI), which is equal to GLS*SF/GS and is 1 when the grains are the same size and shape as the spherical globules.

All the heat-treatment data in Table 3 are represented graphically in Fig. 6. Considering the magnitude of the standard deviations, there is almost no variation in these parameters with temperature and holding time, i.e., the microstructure is time and temperature independent over the semisolid range ($f_l = 0.6 \pm 0.05$) and for all the holding times analyzed (t = 0–120 s). This indicates that the alloy has a chemical composition with sufficient thermodynamic stability to form a homogeneous microstructure without significant fluctuations in size and shape at the semisolid temperature tested (595 °C), an ideal property for adequate control of SSM processing.

The RQI is a maximum of 0.41 ± 0.16 at holding times of 60/90 s. These holding times and a temperature of 595 °C should therefore correspond to the best processing conditions.

Rheological Characterization

The change in the strain versus stress and viscosity versus shear rate curves with holding time for the 355 thixoforged slurries with ~ 40% solid ($f_l = 0.6$) is shown in Fig. 7a and b, respectively. The rheological behavior of the alloy varies little with holding time, as reflected in the very similar curves. Maximum stress values vary from slightly under 5 MPa to just below 6 MPa, much lower than the corresponding figures for conventional cold forming of this type of alloy. The material exhibits homogeneous behavior in the range of holding times tested, although there is an optimal holding time of 30–60 s. At 0 s, i.e., with no holding time, the connections between the primary globules are still strong and greater stress is needed to break them.

The apparent viscosity (Fig. 7b) is also low, reaching a maximum of 1.1 MPa.s and decreasing rapidly to 0.1 MPa.s as the shear rate is increased. In other words, the material has the consistency of melted glass at this temperature. This result is consistent with the literature and can be explained by the marked Ostwald ripening when high heating rates are used in the reheating treatment [1, 2, 5, 18, 19, 23, 25]. For the slurries with an $f_l = 0.6$, there is a small tendency for the viscosity to increase with increasing grain size (Table 3). This can be accounted for by coarsening, which predominates at higher temperatures.

Conclusions

A grain-refined 355 alloy was evaluated by thermodynamic, microstructural, and rheological analysis to assess its potential for use as raw material for SSM processing.

Thermodynamic simulation with Thermo-Calc® and DSC was used to identify an optimal semisolid processing window (T_{SSMI}–T_{SSMF}), which in the worst case (i.e., the narrowest window) was between 592.1 and 621.2 °C. The window identified has low liquid-fraction sensitivity (below 0.03 $°C^{-1}$) and lies between the two thermodynamically

unstable regions in the semisolid range that should be avoided: the eutectic knee (T_{Knee}) and liquidus (T_L).

Microstructural evaluation after partial melting at 595 °C and holding times of 0–120 s revealed a refined, spheroidized microstructure that varied little with temperature and holding time, resulting in highly homogeneous GS, GLS, and CSF for all the conditions tested. GS reached a minimum of 110 μm at 90-s holding time, for which the corresponding GLS and CSF were 77 μm and 0.59, respectively. The stress versus strain and viscosity versus shear rate curves also varied little with holding time. Viscosity was 1.1 MPa.s in the resting state and 0.1 MPa.s under shearing, and a stress of less than 6 MPa was needed to achieve a high deformation (circa ~ 70%).

In general, the results show that 355 alloy is suitable for thixoforming operations, as it has stable microstructural and rheological behavior in the semisolid temperature range when a holding time of 30–60 s is used, a desirable property for adequate control of SSM processing. 355 alloys could be considered an excellent raw material for thixoforming under the right processing conditions.

Acknowledgments The authors would like to thank the *Fundação de Amparo à Pesquisa do Estado de São Paulo* (FAPESP) (Projects 2013-09961-3 and 2015-22143-3), the *Conselho Nacional de Desenvolvimento Científico e Tecnológico* (CNPq) (Projects PQ:306896/2013-3), and *Coordenação de Aperfeiçoamento de Pessoal de Nível Superior* for providing financial support. We would also like to thank the School of Mechanical Engineering at the University of Campinas (UNICAMP).

References

1. D.H. Kirkwood, M. Suéry, P. Kapranos, H.V. Atkinson, K.P. Young, Semi-solid processing of alloys. Springer Ser. Mater. Sci. **124**, 1–172 (2010). https://doi.org/10.1007/978-3-642-00706-4
2. M.C. Flemings, Behavior of metal alloys in the semisolid state. Metall. Trans. A **22A**(5), 957–981 (1991). https://doi.org/10.1007/BF02661090
3. H.V. Atkinson, Modelling the semisolid processing of metallic alloys. Prog. Mater Sci. **50**(3), 341–412 (2005). https://doi.org/10.1016/j.pmatsci.2004.04.003
4. A. Maciel Camacho, H.V. Atkinson, P. Kapranos, B.B. Argent, Thermodynamic predictions of wrought alloy compositions amenable to semi-solid processing. Acta Mater. **51**(8), 2319–2330 (2003). https://doi.org/10.1016/S1359-6454(03)00040-5
5. O. Lashkari, R. Ghomashchi, The implication of rheology in semi-solid metal processes: an overview. J. Mater. Process. Technol. **182**(1–3), 229–240 (2007). https://doi.org/10.1016/j.jmatprotec.2006.08.003
6. G. Chiarmetta, Why thixo? in: Proceedings of the 6th International Conference on Semisolid Processing of Alloys and Composites, Turin, Italy, 15–21 (2000)
7. E.J. Zoqui, M.A. Naldi, Evaluation of the thixoformability of the A332 Alloy (Al–9.5 wt%Si–2.5 wt%Cu). J. Mater. Sci. **46**, 7558–7566 (2011). https://doi.org/10.1007/s10853-011-5730-2
8. Y. Birol, Semisolid processing of near-eutectic and hypereutectic Al–Si–Cu alloys. J. Mater. Sci. **43**(10), 3577–3581 (2008). https://doi.org/10.1007/s10853-008-2565-6
9. D. Liu, H.V. Atkinson, H. Jones, Thermodynamic prediction of thixoformability in alloys based on the Al–Si–Cu and Al–Si–Cu–Mg systems. Acta Mater. **53**(14), 3807–3819 (2005). https://doi.org/10.1016/j.actamat.2005.04.028
10. E.J. Zoqui, Alloys for semisolid processing, in *Comprehensive materials processing*, vol. 5, ed. by J. McGeough (Elsevier Ltd, New York, 2014), pp. 163–190. https://doi.org/10.1016/B978-0-08-096532-1.00520-3
11. E.J. Zoqui, D.M. Benati, C.T.W. Proni, L.V. Torres, Thermodynamic evaluation of the thixoformability of Al–Si alloys. CALPHAD Comput. Coupl. Phase Diagr. Thermochem. **52**, 98–109 (2016). https://doi.org/10.1016/j.calphad.2015.12.006
12. G.L. Brollo, C.T.W. Proni, L.C. de Paula, E.J. Zoqui, An alternative method to identify critical temperatures for semisolid materials process applications using differentiation. Thermochim. Acta **651**, 22–33 (2017). https://doi.org/10.1016/j.tca.2017.02.010
13. E. Tzimas, A. Zavaliangos, Evaluation of volume fraction of solid in alloys formed by semisolid processing. J. Mater. Sci. **35**(21), 5319–5330 (2000). https://doi.org/10.1023/A:1004890711322
14. C.M. Liu, N.J. He, H.J. Li, Structure evolution of AlSi6.5Cu2.8 Mg alloy in semi-solid remelting processing. J. Mater. Sci. **36**(20), 4949–4953 (2001). https://doi.org/10.1023/A:1011804807769
15. H.-S. Kim, I.C. Stone, B. Cantor, Microstructural evolution in semi-solid AA7034. J. Mater. Sci. **43**(4), 1292–1304 (2008). https://doi.org/10.1007/s10853-007-2151-3
16. M. Reisi, B. Niroumand, Growth of primary particles during secondary cooling of a rheocast alloy. J. Alloys Compd. **475**(1–2), 643–647 (2009). https://doi.org/10.1016/j.jallcom.2008.07.090
17. M. Perez, J.-C. Barbé, Z. Neda, Y. Bréchet, L. Salvo, Computer simulation of the microstructure and rheology of semi-solid alloys under shear. Acta Mater. **48**(14), 3773–3782 (2000). https://doi.org/10.1016/s1359-6454(00)00161-0
18. M. Paes, E.J. Zoqui, Semi-solid behavior of new Al–Si–Mg alloys for thixoforming. Mater. Sci. Eng. A **406**(1–2), 63–73 (2005). https://doi.org/10.1016/j.msea.2005.07.018
19. M. Ferrante, E. de Freitas, Rheology and microstructural development of a Al–4 wt%Cu alloy in the semi-solid state. Mater. Sci. Eng. A **271**(1–2), 172–180 (1999). https://doi.org/10.1016/S0921-5093(99)00226-9
20. J. G. Kaufman, E. L. Rooy (2004), Aluminum Alloy Castings. ASM International. ISBN: 0-87170-803-5
21. J.H. Flynn, Analysis of DSC results by integration. Thermochim. Acta **217**, 129–149 (1993). https://doi.org/10.1016/0040-6031(93)85104-H
22. S. Nafisi, R. Ghomashchi, The effect of dissolved titanium on the primary α-Al grain and globule size in the conventional and semi-solid casting of 356 Al–Si Alloy. J. Mater. Sci. **41**(23), 7954–7963 (2006). https://doi.org/10.1007/s10853-006-0866-1
23. C.T.W. Proni, M.H. Robert, E.J. Zoqui, Effect of casting procedures in the structure and flow behaviour of semisolid A356 alloy. Arch. Mater. Sci. Eng. **73**(2), 82–93 (2015)
24. L.V. Torres, L.F. Torres, E.J. Zoqui (2016) Electromagnetic stirring versus ECAP: Morphological comparison of Al–Si–Cu alloys to make the microstructural refinement for use in SSM processing. Adv. Mater. Sci. Eng., Article no. 9789061.1-7. http://dx.doi.org/10.1155/2016/9789061
25. V. Laxmanan, M.C. Flemings, Deformation of Semi-solid Sn-15 Pct Pb Alloy. Metall. Trans. A **11**(12), 1927–1937 (1980). https://doi.org/10.1007/BF02655112